Received: 29 November 2020 | Revised: 18 February 2021 | Accepted: 18 February 2021

DOI: 10.1111/jace.17765

Journal of the American Ceramic Society

ORIGINAL ARTICLE

Effect of structural relaxation on crystal nucleation in a soda-lime-silica glass

Lorena R. Rodrigues[1] | **Alexander S. Abyzov**[1,2] | **Vladimir M. Fokin**[1] | **Edgar Dutra Zanotto**[1]

[1]Graduate Program in Materials Science and Engineering, Department of Materials Engineering, Federal University of São Carlos, São Carlos, Brazil

[2]National Science Center Kharkov Institute of Physics and Technology, Kharkov, Ukraine

Correspondence
Alexander S. Abyzov, Department of Materials Engineering, Center for Research, Technology and Education in Vitreous Materials, Federal University of São Carlos, São Carlos, Brazil.
Email: alexander.abyzov@gmail.com

Abstract

The influence of structural relaxation on crystal nucleation has been underexplored and remains elusive. This article discusses its possible effect on the nucleation process using a stoichiometric soda-lime-silica ($2Na_2O{\cdot}CaO{\cdot}3SiO_2$) glass as a model system. We show that the relaxation effect is powerful at low temperatures, close and below the glass transition, T_g, and leads to a continuous increase in the nucleation rate. At any given temperature, the nucleation rate eventually reaches its ultimate steady-state corresponding to the fully relaxed supercooled liquid (SCL). However, the time to reach the steady-state is two to three orders of magnitude *longer* than the average relaxation time estimated by the Maxwell relation (shear viscosity / shear modulus). The proposed nucleation mechanism and model, which take relaxation into account, and related experimental results also explain the alleged "breakdown" of CNT at low temperatures reported for various glasses. It confirms a few recent papers that this apparent flaw is merely because most researchers did not prolong nucleation treatments enough to complete the relaxation process to achieve a steady state. Another remarkable result is that the actual maximum nucleation temperature, T_{max}, is significantly lower than the previously reported values. Finally, a comparative analysis of the kinetic coefficient using viscosity versus growth velocity favors the last. These results for this soda-lime-silica glass extend and validate recent findings for lithium disilicate on the significant (but often neglected) effect of relaxation on crystal nucleation.

KEYWORDS

crystal growth, glass, glass transition, nucleation, phase transition, relaxation

1 | INTRODUCTION

Avoiding or controlling crystallization of supercooled glass-forming liquids underpins the development of glasses and glass-ceramics, respectively.[1,2] Yet on this topic, the Classical Nucleation Theory (CNT) is often used to analyze and predict crystal nucleation kinetics.[3,4] For temperatures above the temperature T_{max} of the maximum nucleation rate, $I(T)$, observed in common experiments, which is near the glass transition range, experimental nucleation data can be described in the CNT framework. However, for temperatures below T_{max}, the theory predicts much *higher* nucleation rates than the experimentally observed values. This discrepancy between theory and experiment, known as the "breakdown" of CNT (hereafter we will use a more adequate term "apparent breakdown"), strongly increases with decreasing temperature.

Various possible reasons to explain this disagreement have been proposed in recent years[5-10] with limited success. In particular, in Ref. 5-7 significant structural changes in the supercooled liquid with a decrease in temperature, which could affect the nucleation process, were advanced. Since T_{max} is usually located within the glass transition interval

(corresponding to very high viscosity), structural relaxation at $T < T_{max}$ could affect the nucleation process. This effect was recently shown experimentally and was theoretically analyzed for a lithium disilicate (LS2) glass in Ref. 11,12. These two works demonstrated that the crystal number density versus time, $N(t)$, curves *cannot* be described in the CNT framework using a constant set of diffusion coefficient and interfacial energy. Since these parameters depend on the liquid state, this result gives evidence for the structural relaxation that results in an increase in the nucleation rate. The latter only achieves the theoretically expected steady-state value when the supercooled liquid (SCL) fully relaxes, that is, reaches the final metastable state corresponding to the given temperature.

The present work aims to analyze two sets of new and old nucleation data using a glass of nominal composition $2Na_2O{\cdot}CaO{\cdot}3SiO_2$ ($N_2C_1S_3$) as a model system, taking into account the effect of structural relaxation, which was only discussed so far for lithium disilicate glass.[11] The objective is to generalize (or not) the scarcely considered effect of relaxation on crystal nucleation employing an advanced analysis of nucleation data compared with that used in Ref. 11. We also improve the model by taken into account the effect of relaxation on the diffusivity, D (in the previous two articles[11,12] on LS_2, only the effect on the driving force, ΔG_V, was studied). Finally, we aim to test whether the viscosity or crystal growth velocity best describes the kinetic coefficient in crystal nucleation.

2 | MATERIALS AND METHODS

The effect of relaxation on crystal nucleation in lithium disilicate (LS_2) glass was focused on in previous research.[11] In this work, the $2Na_2O{\cdot}CaO{\cdot}3SiO_2$ ($N_2C_1S_3$) glass was chosen as a model system to validate and extend the findings with LS_2 because it also shows internal homogeneous nucleation in a wide range of temperatures, and has been much less studied than other options, such as barium silicate glasses. The glass was prepared according to the procedure described in Ref. 10, where detailed information about glass melting, quenching, and characterization can be found. Its chemical composition in mole % ($32.86Na_2O{\cdot}17.40CaO{\cdot}49.74SiO_2$) is close to the nominal one ($33.33Na_2O{\cdot}16.67CaO{\cdot}50.00SiO_2$). Its glass-transition temperature, T_g, estimated from a DSC heating curve is 747 K.

Nucleation and growth heat treatments were carried out in a vertical electrical furnace with a pre-stabilized temperature within ±1 K. The time dependence of the crystal number density, $N(t)$, at several nucleation temperatures, T_n, was measured using the Tamman method.[13] This technique consists of growing nuclei, previously formed at T_n, up to a detectable size at the development temperature, T_d. This temperature must meet the following requirements: $I(T_d) \ll I(T_n)$ and $U(T_d) \gg U(T_n)$, where U is the growth velocity. Samples were subjected to nucleation treatments at T_n= 719, 729, and 808 K and then to "development" treatments at T_d = 843K. Moreover, some $N(t)$ curves for nucleation temperatures between 738 to 793 K determined in Ref. 10 for samples of the same glass batch were extended to longer time periods.

After the heat treatments, the samples were polished with SiC paper and a CeO_2 suspension to remove the surface crystallized layer. Then, cross sections were analyzed by reflected light optical microscopy (LEICA DMRX coupled to a LEICA DFC490 camera) to measure the number of crystal intersections and the radius of the largest crystal, which is equal to the radius of the largest crystal inside the sample.

It should be noted that the development method practically yields a mono dispersed crystal size distribution in the sample´s interior. Therefore, the crystal number density, N_V, after treatment at T_d was estimated as

$$N_V = \frac{N_S}{2R}, \tag{1}$$

where N_S is the number of crystal traces in a sample cross section of area S, and R is the maximal radius of the crystals in the cross sections (see, e.g., Ref. 14). As this technique could underestimate the number N_S in the cross sections (due to the limited resolution limit of the optical microscope), the following equation was used to correct for the underestimated fraction, f,[13]

$$f = \frac{2}{\pi}\sin^{-1}\frac{\varepsilon}{D_M}, \tag{2}$$

where ε is the resolution limit of the microscope (0.5 μm) and D_M is the diameter of the largest crystal in the cross section. Hence, the corrected N was given by Eq. (3)

$$N = \frac{N_V}{1-f}, \tag{3}$$

where N_V is the measured crystal density and N the corrected value.

To estimate the crystal growth velocity, $U(T)$, single-stage heat treatments for various times at each growth temperature (793-883 K) were performed. As the $2Na_2O{\cdot}CaO{\cdot}3SiO_2$ crystals have a spherical shape (Figure 1), a linear fit to the time dependence of the radius of the *largest* crystal, R_M, in micrographs of the sample cross-sections, which coincide with the real size of the largest crystal, was used to evaluate $U(T) = dR_M/dt$.

The structural relaxation kinetics was studied by following the variation in the refractive index, n_λ, with the time of isothermal treatment. Before the measurements, a sample

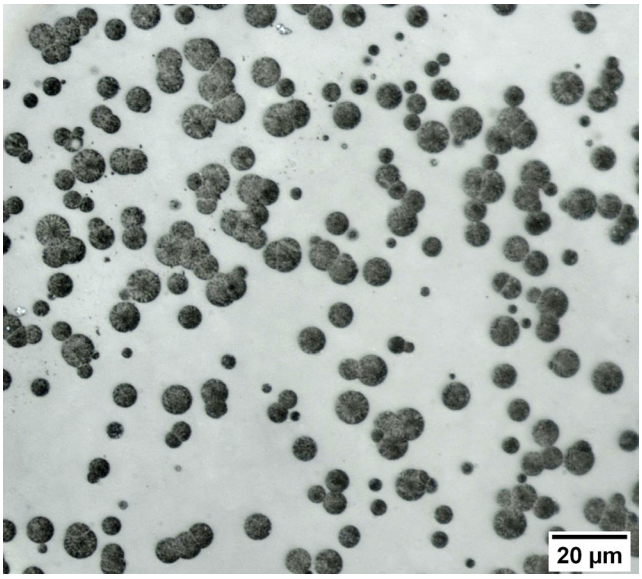

FIGURE 1 Reflected light optical micrograph of a cross section of a $N_2C_1S_3$ glass sample treated for 30 min at 843 K showing spherical crystals. The variation in the cross-section sizes is because crystals are cut at different parts. The largest ones were cut in their centers [Color figure can be viewed at wileyonlinelibrary.com]

of ~10 × 10 × 2.5 mm, with two perpendicularly polished faces, was kept for 70 minutes at 5 K below the DSC T_g to fix the initial fictive temperature, T_f. Then, the same sample was subjected to isothermal treatments at 729 K ($T_f - 13$K). After each heat treatment, it was removed from the furnace and held for 20 minutes, to stabilize it at room temperature. Then the refractive index measurement was performed.

The refractive index was determined using a Pulfrich refractometer with a spectral mercury lamp (monochromatic green e-line, λ = 546.1 nm) and a Vo F5 prism (refractive index $n_p = 1.748005$). The refractometer measures the angle of the refracted beam, γ, which is related to n_λ by the following equation:

$$n_\lambda^2 = n_p^2 - \cos\gamma \cdot \sqrt{n_p^2 - \cos^2\gamma}. \quad (4)$$

3 | GOVERNING EQUATIONS

According to CNT, the steady-state nucleation rate in equilibrium SCL can be written as[15,16]

$$I_{st}(T) = \frac{1}{d_0^3}\sqrt{\frac{\sigma_{eq}}{kT}}\frac{2D}{d_0}\exp\left(-\frac{W_{c,eq}}{k_BT}\right), \quad (5)$$

where D is the effective diffusion coefficient, $W_{c,eq}$ is the thermodynamic barrier for nucleation or the work of formation of a nucleus of critical size, R_c, σ_{eq} is the surface tension of the critical nucleus/SCL interface, d_0 is the effective size of the structural units—commonly estimated as $d_0 = \left(\frac{V_M}{N_A}\right)^{1/3}$ via the crystal molar volume, V_M, and the Avogadro number, N_A—k_B is the Boltzmann constant, and $T$is the absolute temperature. For our particular substance ($N_2C_1S_3$ glass) $d_0 = 0.6$nm.

In the case of the spherical nucleus

$$R_c = 2\sigma_{eq}/\Delta G_{V,eq}, \quad (6)$$

$$W_{c,eq} = \frac{16}{3}\pi\frac{\sigma_{eq}^3}{\Delta G_{v,eq}^2}, \quad (7)$$

where $\Delta G_{V,eq}$ is the thermodynamic driving force for crystallization for the fully relaxed, metastable state of the supercooled liquid, which can be estimated via the following polynomial

$$\Delta G_{V,\,eq}(T) = 1.5148 \cdot 10^8 + 112585.1 \cdot T - 149.566 \cdot T^2, \quad (8)$$

with temperature T in Kelvin and ΔG_v in J/m^3 (this polynomial describes thermodynamic data for the $N_2C_1S_3$ glass well[13]).

To estimate $\sigma_{eq}(T)$, we use Tolman's equation

$$\sigma_{eq}(T) = \frac{\sigma_0}{1 + \frac{2\delta}{R_c(T)}}, \quad (9)$$

where σ_0 is the surface tension of a planar interface, and δ the Tolman parameter, which is of the order of the crystal unit-cell.

As follows from Eq. (5), the effective diffusion coefficient D is one of the key parameters to evaluate the nucleation kinetics. Following our previous article,[11] we estimate D from the crystal growth rate given by Eq. (10),[17] for the Screw Dislocation model, which is the most frequent growth mechanism in glass-forming liquids

$$U = \frac{T_m - T}{2\pi T_m} \cdot \frac{D_U}{4d_0}\left[1 - \exp\left(-\frac{\Delta G_{V,eq} d_0^3}{k_BT}\right)\right], \quad (10)$$

where T_m is the melting point.

Thus, in our calculations, we reasonably assume that $D = D_U$. That is, the same diffusion coefficient determines both nucleation and crystal growth, since they refer to a single process of diffusion. In the Appendix, we show a comparison of D_U with $D\eta$, calculated from viscosity, which is an approximation normally used in nucleation studies.

Also, several authors, for example, Ref. 3, including ourselves,[5,18,19] *incorrectly* (as was shown in Ref. 11 for the LS_2 glass, and will be further shown in this article for the current glass) estimated D from the apparent nucleation induction time, t_{ind}, or the nucleation time-lags, τ, interpreting the nucleation rate increase with time as a classical nonstationary nucleation. At deep supercoolings, where homogeneous

nucleation rates can be detected in laboratory scales, the temperature range used in this research work, $U(T)$ shows an Arrhenian behavior (as shown, e.g., in Figure 2):

$$U = U_0 \exp\left(-\frac{E_U}{k_B T}\right), \tag{11}$$

where U_0 is a pre-exponential term and E_U the activation energy for crystal growth.

Since the thermodynamic term in Eq. (10) is negligible at deep supercoolings, Eqs. (10) and (11) yield the following relation for D_U:

$$D_U = \frac{8\pi d_0 U_0 T_m}{T_m - T} \exp\left(-\frac{E_U}{k_B T}\right). \tag{12}$$

To take into account the effect of glass structural relaxation on the nucleation rate, we introduce a factor $\zeta(t)$ into the thermodynamic driving force for crystallization

$$\Delta G_V(T, \zeta) = \Delta G_{V,\,eq}(T)\,\zeta(t), \tag{13}$$

that correlates with the structural order-parameter, ξ, as

$$\zeta = 1 + \left(\frac{\xi - \xi_{eq}}{\xi_{eq}}\right)^2. \tag{14}$$

The subscript *eq* indicates that the value refers to a fully relaxed equilibrium liquid, SCL (a detailed theory is given in Ref. 12).

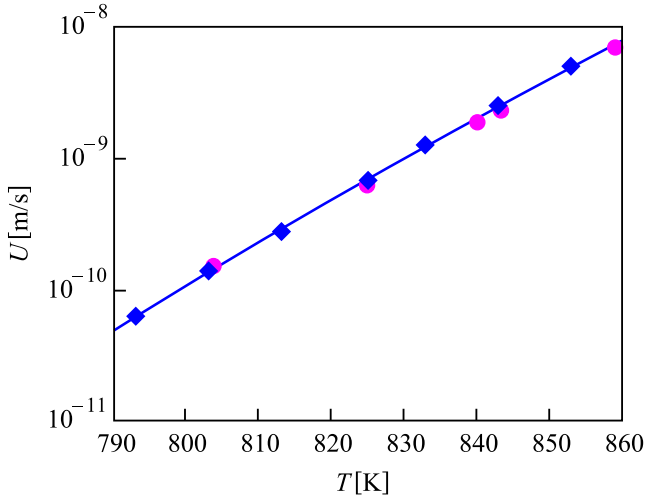

FIGURE 2 Temperature dependence of the crystal growth velocity at deep supercoolings. Rhombuses and circles represent experimental data for the current glass batch and from[21], respectively. The solid line refers to an Arrhenius fit, Eq. (11), to the data of this work [Color figure can be viewed at wileyonlinelibrary.com]

According to the Stefan–Skapski–Turnbull relation, the surface tension of a crystal/liquid interface is proportional to the heat of melting per particle q

$$\sigma_{eq} = \alpha \frac{q}{d_o^2}. \tag{15}$$

Since for $N_2C_1S_3$ glass, the thermodynamic driving force for crystallization is very close to the value calculated by the Hoffman approximation,[13] Eq. (15) can be rewritten as

$$\sigma_{eq} = \alpha \Delta G_{V,eq} d_0 \frac{T_m}{T}\left(1 - \frac{T}{T_m}\right)^{-1}. \tag{16}$$

Under the assumption that Eq. (16) is also valid in the case of a non-equilibrium liquid during its structural relaxation, Eqs. (13) and (16) yield

$$\sigma(\zeta) = \sigma_{eq}\zeta. \tag{17}$$

Employing Eqs. (13) and (17), we obtain the dependence of the work of critical cluster formation on the parameter ζ

$$W_c(\zeta) = W_{c,eq}\zeta. \tag{18}$$

Finally, we can write the following equation for the nucleation rate in a relaxing glass or SCL

$$I_{st}(T,t) = \frac{1}{d_0^3}\sqrt{\frac{\sigma_{eq}(T)\,\zeta(t)}{kT}}\frac{2D(T,t)}{d_0} \exp\left(-\frac{W_{c,eq}(T)\,\zeta(t)}{k_B T}\right), \tag{19}$$

$$D(T,t) = \frac{8\pi d_0 U_0 T_m}{T_m - T} \exp\left(-\frac{E_U \zeta(t)}{k_B T}\right). \tag{20}$$

It should be noted that, unlike our previous similar analysis,[11] here structural relaxation of the glass determines the change, not only in the thermodynamic nucleation barriers, but also the change in the diffusion activation energy, E_U.

The time evolution of ζ can be approximated by an exponential law

$$\zeta(t,T) = 1 + \zeta_0(T) \cdot \exp\left(-\frac{t}{\tau_{sr}(T)}\right), \tag{21}$$

where τ_{sr} represents the characteristic time of the structural relaxation process related to crystal nucleation

Relaxation is completed when $\zeta = 1$ and, hence, the nucleation rate reaches its final steady-state value predicted by CNT at any given temperature.

4 | RESULTS

4.1 | Diffusivity

Figure 2 shows the crystal growth velocity data, $U(T)$, of this and a previous study,[20] and an Arrhenius fit (Eq. (11)), with the following fitting parameters:

$$U_0 = 5.84 \cdot 10^{16}\text{m/s}, \quad E_U = 6.8 \cdot 10^{-19}\text{J}, \tag{22}$$

The growth velocity data for the current glass batch are quite close to the old data for a glass of similar composition ($34.04Na_2O{\cdot}15.51CaO{\cdot}50.45SiO_2$ mole %),[20] which is also close to the nominal composition.

To compare D_U with the diffusion coefficient for viscous flow, D_η, we fitted the temperature dependence of the shear viscosity data, $\eta(T)$, for the *same* glass batch used in the nucleation and growth experiments using the classical VFT equation

$$\eta = \eta_0 \exp\left[-\frac{E_\eta}{k_B\left(T - T_0\right)}\right], \tag{23}$$

where $\eta_0 = 4 \cdot 10^{-9}\ \text{m}^2\text{s}^{-1}$, $E_\eta = 1.69 \cdot 10^{-19}\text{J}$, and $T_0 = 485.64\text{K}$.

Figure 3 shows the experimental $\eta(T)$ data and the Arrhenius fit.

The diffusion coefficient, D_η, obtained via the Stokes–Einstein–Eyring equation[15]

$$D_\eta(T) = \frac{k_B T}{\kappa d_0 \eta(T)}, \tag{24}$$

and D_U (Eq. (12)) are shown in Figure 4. In Eq. (24) the coefficient $\kappa = 0.258$ yields $D_\eta(T) = D_U(T)$ at high temperatures, above the temperature T_{dec}, at which the well-known decoupling between D_η and D_U takes place.[21,22]

The Appendix shows a discussion on which of these parameters is most adequate for analyzing nucleation kinetics, which indicates that, when relaxation is significant, the N vs t curves are best described by D_U.

4.2 | Structural Relaxation versus Nucleation Kinetics

Figure 5 shows the crystal number density $N(t)$in glass samples subjected to nucleation treatments at T_n=719-808 K for time t, followed by a "development" treatment at $T_d = 843\text{K}$. Points correspond to the experimental data. The $N(t)$dependences denoted by solid blue lines were calculated from fitting experimental data with the equation

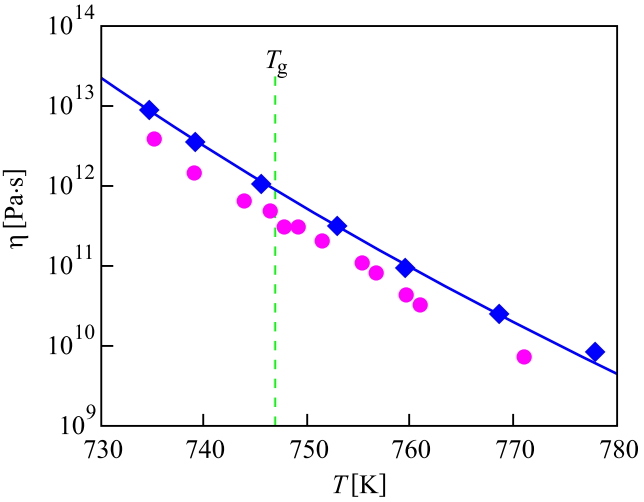

FIGURE 3 Temperature dependence of the shear viscosity. Rhombuses and circles refer to experimental data from[10] and[21], respectively. The difference between the two sets of experimental data could be associated with small compositional differences and using different methods: "penetration"[10] and "beam bending"[21]. The solid line was obtained from fitting Eq. (23) to the data of[10], which refers to the glass used in this work. The vertical line shows the DSC T_g of the current glass, which is close to the typical viscosity of 10^{12} Pa·s [Color figure can be viewed at wileyonlinelibrary.com]

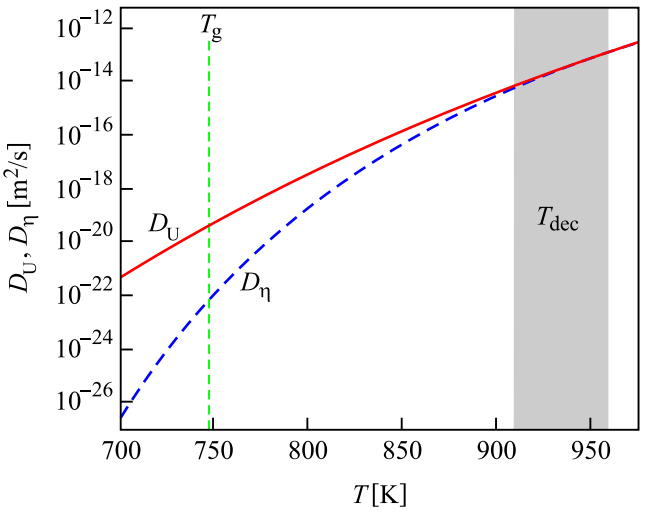

FIGURE 4 Diffusion coefficients estimated from the crystal growth velocity, D_U (solid line, Eq. (12)), and viscosity, D_η (dashed line, Eq. (24)) showing the classical decoupling starting at 910-960 K. [Color figure can be viewed at wileyonlinelibrary.com]

$$N(t) = \int_0^t I\left(t'\right) dt', \tag{25}$$

where the nucleation rate, $I(t)$, is determined by Eqs. (19)-(21) and (9).

The parameters σ_0 and δ in Eq. (9) were obtained by fitting the experimental nucleation rates, I_{st}, measured at

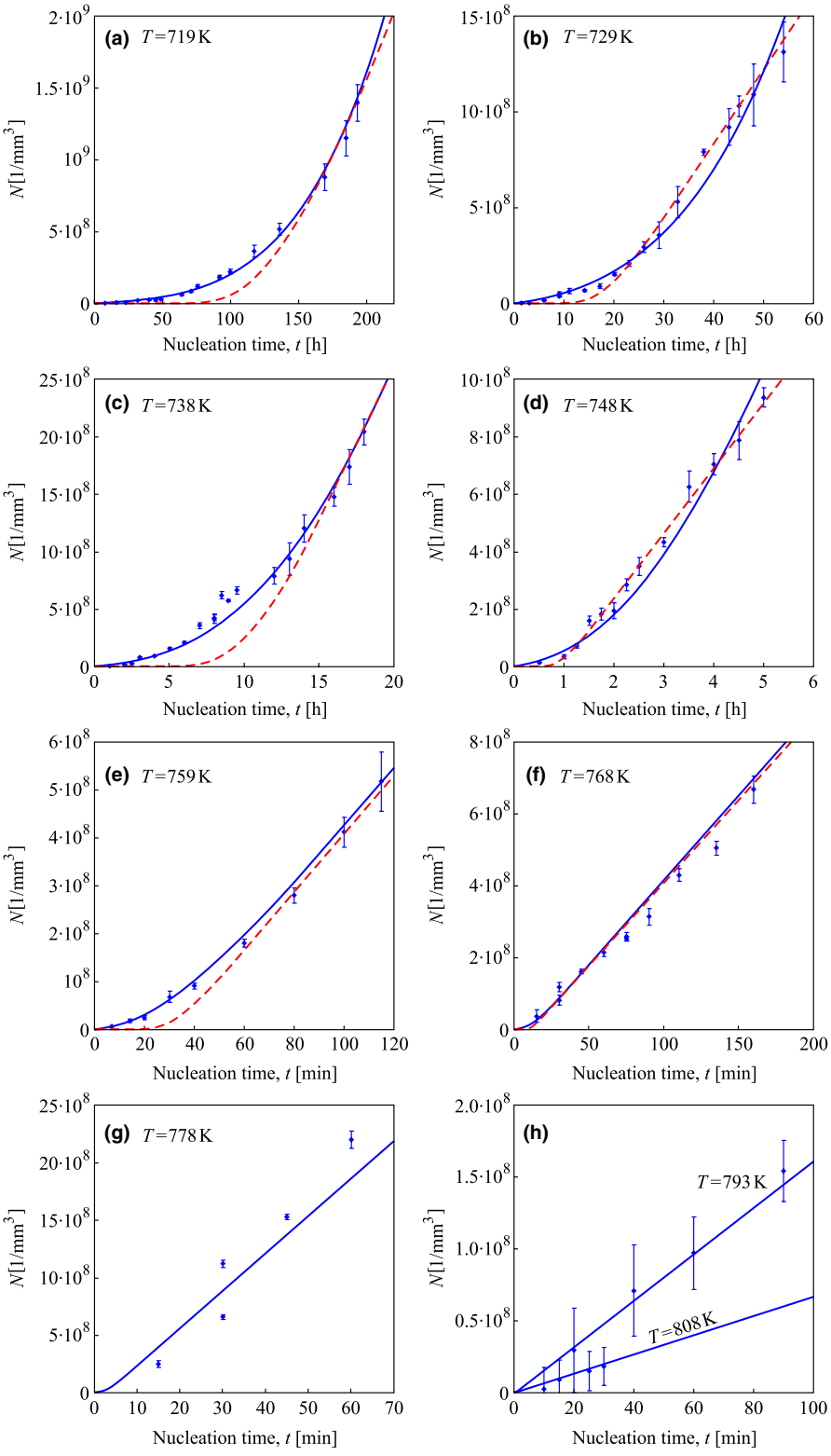

FIGURE 5 Number of crystals per unit volume, $N(t)$, versus nucleation time, t, for different temperatures. The symbols represent experimental data, whereas the solid blue lines show fits via Eqs. (19), (20), (21), and (9). The dashed red lines were obtained via simulations based on the cluster dynamics model with time independent D and σ, which were the fitting parameters that best describe the final part of the experimental $N(t)$ dependences. The dashed red lines in G and H coincide with the solid blue lines [Color figure can be viewed at wileyonlinelibrary.com]

temperatures *above* the experimental T_{max}, $T = 768\ldots808\text{K}$, where we assume $\zeta = 1$ due to the very fast structural relaxation in this temperature range. From such fitting, the values of σ_0 and δ are: $\sigma_0 = 0.1738\ \text{J}/\text{m}^2, \delta = 0.99\ d_0$.

Fitting with Eq. (25) yields the values of parameters ζ_0 and τ_{sr} to achieve the best agreement with the experimental $N(t)$ dependence. The fitting results are presented in Table 1.

It should be noted here that in the case of $2Na_2O{\cdot}CaO{\cdot}3SiO_2$ glass, the effect of the development temperature T_d on the $N(t)$ dependence due to dissolution of crystals with a size smaller than the critical one corresponding to T_d can be neglected because of the fast diffusion (and growth rates) at nucleation temperatures. Therefore, a change in the development temperature from

TABLE 1 Parameters ζ_0 and τ_{sr} obtained from fitting experimental data to Eq. (25), nucleation time-lags, τ_K, estimated by Eq. (31), and Maxwell times, τ_M, calculated by Eq. (30) for different temperatures

T [K]	ζ_0	τ_{sr}[s]	τ_K[s]	τ_M[s]	τ_{sr}/τ_K	τ_{sr}/τ_M
719	0.077	$8.5 \cdot 10^5$	163	9872	5207	86
729	0.053	$2.3 \cdot 10^5$	65.1	1144	3476	198
738	0.04	$4 \cdot 10^4$	29.14	190	1367	210
748	0.029	7308	12.21	30	599	244
759	0.021	1422	4.82	4.58	295	310
768	0.021	472	2.3	1.1	205	429
778	0.021	100	1.03	0.25	97	400
793	0.021	15.5	0.322	0.032	48.1	484
808	0.021	2.87	0.105	0.005	27.3	574

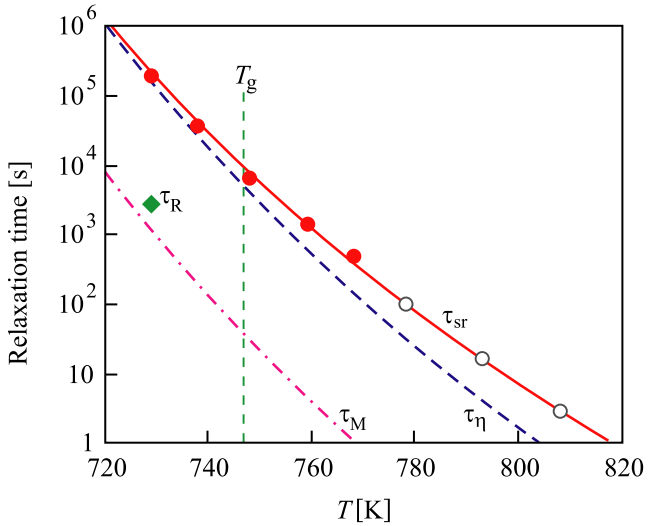

FIGURE 6 Relaxation times versus temperature. The full and empty red circles indicate the characteristic times τ_{sr} of structural relaxation calculated from nucleation data (see Eq. (21)) and extrapolated to high temperatures, respectively. This extrapolation is necessary for calculations with Eqs. (19)-(21). The solid line represents a fit via Eq. (26), the dashed line shows the relaxation times estimated from viscosity, τ_η (Eq. (28)), and the dot-dashed line shows Maxwell's relaxation times, τ_M, evaluated by Eq. (30). The Rhombus indicates the τ_R estimated from relaxation of the refractive index, Eq. (29) [Color figure can be viewed at wileyonlinelibrary.com]

843 K to 923 K does not lead to a noticeable decrease in the number N of developed crystals.

The dashed red lines in Figure 5 were obtained by calculation of the time-dependent cluster size distribution function. It is done from a set of coupled linear differential equations that describe reactions of attachment and detachment of single molecules ("structural units") to or from clusters of a new phase (more details of the *Cluster Dynamics Model* are given in Refs. 3,16). D and σ listed in Table A1 were used as fitting parameters for the best description of the *final part* of the

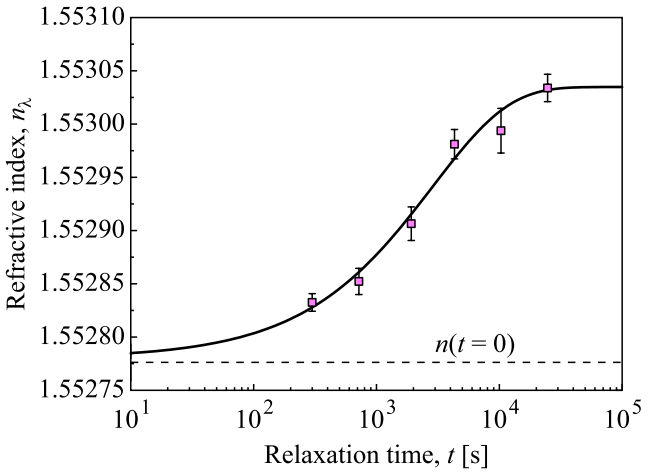

FIGURE 7 Refractive index of the current soda-lime-silica glass versus treatment time at 729 K. The line is a fit by Eq. (29) [Color figure can be viewed at wileyonlinelibrary.com]

experimental time dependences $N(t)$. Below we will discuss the incorrectness of such fitting procedure performed for a limited time interval, shown also in[11].

Figure 6 shows the characteristic structural relaxation times, τ_{sr}, obtained from the nucleation curves:

$$\tau_{sr}(T) = \tau_0 \exp\left[-\frac{E_\tau}{k_B(T - T_0)}\right], \tag{26}$$

$$\tau_0 = 1.3 \cdot 10^{-16}\text{s}, \quad E_\tau = 1.48 \cdot 10^{-19}\text{J}. \tag{27}$$

The characteristic relaxation times calculated from viscosity

$$\tau_\eta(T) = \frac{d_0^2}{D_\eta(T)}, \tag{28}$$

where $D_\eta(T)$ is determined by Eq. (24), and the characteristic time of the refractive index relaxation τ_R (see Eq. (29)) also presented in Figure 6.

The time evolution of the refractive index at 729 K is shown in Figure 7. The line is a fit by Eq. (29)., that is, the Kohlrausch stretched exponent expression:

$$n_\lambda = n_{\lambda,inf} + (n_{\lambda,0} - n_{\lambda,inf}) \exp\left[-\left(\frac{t}{\tau_R}\right)^\beta\right] \tag{29}$$

with $n_{\lambda,0} = 1.55278$, $n_{\lambda,inf} = 1.55303 \pm 1.3 \cdot 10^{-5}$, $\tau_R = (2860 \pm 600)\,s$, and $\beta = 0.70 \pm 0.08$.

For the sake of comparison, we calculated the Maxwell relaxation times

$$\tau_M = 2\frac{\eta(1+\gamma)}{E}, \tag{30}$$

where the Young modulus $E = 71\text{GPa}$ and Poisson's ratio $\gamma = 0.23$ were used as typical values for silicate glasses. Equation (30) gives a lower boundary of the characteristic alpha relaxation times, τ_R, of some glass properties, such as density or refractive index.[23] Indeed, the experimental value of τ_R is slightly higher than the calculated value of τ_M (Figure 6).

5 | DISCUSSION

As we indicated in the Introduction section, the main objective of the present work using $N_2C_1S_3$ glass was to *generalize the strong effect of structural relaxation on the nucleation kinetics below* T_{max}, which were first described in our recent article for lithium disilicate glass.[11] This problem is very relevant because the CNT and other theories assume that nucleation takes place in a fully relaxed SCL. Moreover, it deals with a well-known, long-standing problem—the CNT "apparent breakdown"—which is quite considerable at low temperatures corresponding to the glass transition range and below.

The dependences of the number of nucleated crystals, $N(t)$, on the nucleation time, required for any in-depth analysis of the nucleation kinetics, are shown in Figure 5 for $N_2C_1S_3$ glass, where the symbols represent experimental data. These data cannot be described within the framework of CNT using a constant set of parameters at any given temperature, as we have already demonstrated for lithium disilicate glass.[11] This fact is illustrated by the red dashed lines, simulated via the *Cluster Dynamics Model*, employing D and σ_{eq} as fit parameters to achieve the best agreement with the *final* parts of the N versus t curves in Figure 5. These dashed lines describe only the time interval selected for fitting and are far below the experimental data corresponding to the previous parts, especially the very beginning of the $N(t)$ plots.

The impossibility to describe the full N versus t experimental curves with a constant set of parameters led us to suggest that they *change over time*. Such changes are due to the continuous structural relaxation of the glass, which brings it closer to the fully relaxed metastable state of the supercooled liquid. Thus, the fitting procedure of a limited part of the $N(t)$ dependence is incorrect because it does not take into account the previous change in the system parameters and, as a consequence, it cannot be used to estimate the diffusion coefficient and interfacial energy determining the nucleation process. An exception is at the very beginning of the $N(t)$ curve, when it is possible to neglect changes in the glass structure, and hence adopt the CNT. Our analysis also shows that a higher value of diffusion coefficient (than the value resulting from fitting the final part of the curve) is needed to describe the initial part of the $N(t)$ dependence. For this reason, following Ref. 11, to analyze the nucleation rates we used the *diffusion coefficients determined from the growth velocities* via Eq. (12), assuming that similar diffusion coefficients govern both crystal nucleation and crystal growth.

Equations (9), (19)-(21) allow us to describe the $N(t)$ data within the framework of the proposed model taking into account the effect of structural relaxation in the nucleation kinetics. To achieve the best possible agreement with experimental data, ζ_0 and τ_{sr} were used as fitting parameters (Table 1).

Figure 6 shows a clear correlation between the characteristic nucleation times, $\tau_{sr}(T)$, and $\tau_\eta(T)$ estimated from shear viscosity by Eq. (28), similar to what we observed earlier for lithium disilicate glass[11]. It gives indirect evidence of the similar influence of the elementary structural rearrangements on both viscous flow and nucleation. However, it should be emphasized that it is related to the *relaxation* process, which results in the change in thermodynamic barrier for nucleation, W_c, and effective diffusion coefficient, D, and hence is responsible for the evolution of nucleation kinetics. To evaluate the latter, we used D_U rather than D_η. Thus D_η seems to determine the relaxation process, whereas D_U controls the nucleation rate (see a discussion in the Appendix).

When comparing these different relaxation times, it should be emphasized that the Maxwell relaxation times, τ_M, are 2-3 orders of magnitude *shorter* than the relaxation times, τ_{sr}, determined directly from nucleation experiments (see Table 1). This fact is consistent with measurements of the characteristic time, τ_R, of refractive index relaxation, which completes well before the nucleation relaxation process, τ_{sr}, which underlies the crystal nucleation kinetics (Figure 6). A similar result was recently obtained[11] based on the density relaxation of lithium disilicate glass. Thus, the relaxation process underlying nucleation is *different* from Maxwell's relaxation, or the traditional alpha-relaxation inferred by density or refractive index variations, and warrants a more in-depth analysis.

To answer the question of whether the stationary nucleation regime had enough time to be reached during this long relaxation process, we calculated the classical nucleation time-lag, τ_K, by Eq. (31),[24] for several temperatures with the *approximation* $D = D_U$ (see Table 1).

$$\tau_K = \frac{16}{3}\frac{\sigma k_B T}{D d_0^2 \Delta G_v^2}. \tag{31}$$

The ratio τ_{sr}/τ_K listed in Table 1 decreases with temperature, but is much greater than one in the temperature interval of the nucleation experiments. It means that, *if* the diffusion coefficient controlling nucleation is the *same* as the one that controls crystal growth, nucleation would reach the steady-state regime well before structural relaxation was completed.

In other words, at each moment of time (except the initial interval $t < 3\tau_K \ll \tau_{sr}$ [24]), the nucleation rate is close to the stationary value corresponding to the given state of liquid. After the structural relaxation process is completed, the nucleation rate reaches its *ultimate* steady-state value corresponding to the given temperature. Thus, the increase in the nucleation rate over time is a consequence of the structural relaxation of liquid but is *not* the classical nonstationary nucleation described by CNT, which has been interpreted over the last 50 years (e.g., [3,13]). Note that this interpretation also led to an incorrect determination of the diffusion coefficient, since the relaxation process was understood as being a classical nonstationary nucleation and, as a consequence, this resulted in an artificial problem of decoupling between the diffusion coefficients estimated from nucleation and growth rates.[25]

The slow structural relaxation at temperatures at and below the glass transition interval results in deviations of the glass or intermediate liquid state from the metastable equilibrium. As a result, during conventional experiments at these temperatures, due to short nucleation treatment times typically used, the measured nucleation rate is often less than its ultimate steady-state value corresponding to the fully relaxed metastable equilibrium liquid.

The choice of the maximal duration of nucleation experiments, which is related to the time needed to reach the final linear part of $N(t)$ dependence, is limited by the maximum crystal number density, N_{max}, that can be experimentally determined (due to the limited resolution of the available microscope). This case of not reaching N_{max}, often happens for glasses displaying very high nucleation rates. For example, in the case of the current $N_2C_1S_3$ glass at the temperature of the theoretically predicted maximum nucleation rate $T_{\text{tmax}} = 720\text{K}$ (estimated by curve 6 in Figure 8) the time, $t_{0.93}$, when the nucleation rate approaches its ultimate steady-state value, $I_{st}\left(T_{\text{tmax}}, t_{0.93}\right)/I_{st}\left(T_{\text{tmax}}, \infty\right) = 0.93$, is equal to 886 hours (~37 days), and the crystal number density would be $N = 2.5 \cdot 10^{11}\text{mm}^{-3}$, which corresponds to an average crystal-crystal distance of ~160 nm. This small distance is not resolvable by an optical microscope; therefore, such high crystal density cannot be measured by optical microscopy.

Figure 8 illustrates the relativity of the temperature dependence of the nucleation rate $I(T)$ if the maximum nucleation time (limited by the microscope resolution or by the lack of patience of the researcher) is insufficient to complete the relaxation process, hence to reach the ultimate steady-state nucleation rate. The blue rhombuses represent the nucleation rates estimated from the *final parts* of the $N(t)$ dependences shown in Figure 5. The red points were taken from a previous paper[20] on a glass of the same nominal composition. Line 6 was plotted via Eqs. (19) and (20) with $\zeta = 1$ (relaxation process completed), which corresponds to the real temperature dependence. Lines 1, 2, 3, 4, and 5 show $I(T,t) = dN(t)/dt$ taken from N vs t curves plotted via Eqs. (19)-(21) up to a

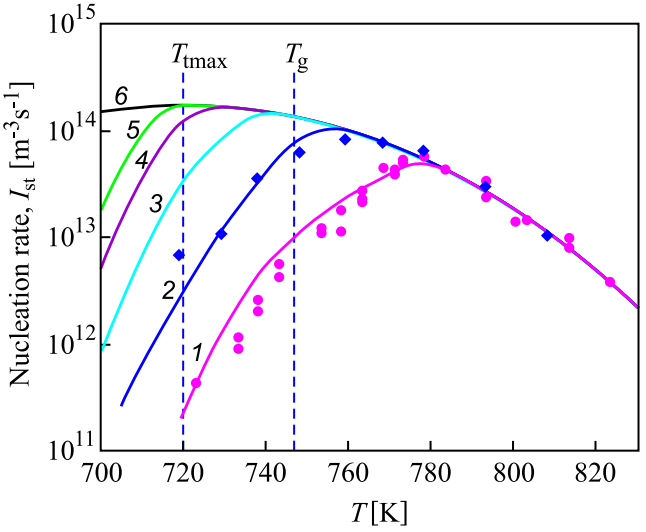

FIGURE 8 Temperature dependence of the "apparent" steady-state nucleation rates of $N_2C_1S_3$ glass. The vertical line at T_{tmax} shows the location and value of the theoretically predicted maximum nucleation rate. The blue rhombuses show the results of this work, including $N(t)$ data reported in[10] for the same glass batch, whereas the magenta circles show our previous results[20] for another glass batch of the same nominal composition, in which the heat treatments were much shorter. The lines are plotted via Eqs. (19) and (20), line 6 considers $\zeta = 1$ (full relaxation), whereas lines 1, 2, 3, 4, and 5 indicate $I_{st}(T)$ predictions for the times when the maximum value of $N(t)$, N_{max}, reached 10^7, $5 \cdot 10^8$, 10^{10},10^{11}, and $5 \cdot 10^{11}\text{mm}^{-3}$, respectively [Color figure can be viewed at wileyonlinelibrary.com]

time t, when $N(t)$ reached values of 10^7, $5 \cdot 10^8$, 10^{10}, 10^{11} and $5 \cdot 10^{11} mm^{-3}$, respectively. For the lines 1-4, the times used were *not* sufficient to complete the relaxation process at the lowest temperatures, therefore the computed nucleation rates were lower than the ultimate steady-state nucleation rates (denoted by line 6). Since the relaxation time strongly decreases with an increasing temperature, from a certain temperature the used experimental times become sufficient for complete relaxation and, hence, for reaching the ultimate steady-state nucleation rate. This temperature corresponds to that of the apparent (experimental) nucleation rate maximum, above which the experimental and theoretical nucleation rates coincide.

Figure 8 shows that the apparent maximum nucleation rates approach the theoretically calculated maximum as the maximal number of crystals increases (due to the increase in nucleation treatment time) and achieve it when $N = 5 \cdot 10^{11}\text{mm}^{-3}$ (see line 5). Comparing the new and old nucleation rates of the $N_2C_1S_3$ glass, it can be observed that, in the latter case, the maximal number of crystals, $N(T)$, is approximately one order of magnitude less than the first. This fact is the origin of the differences observed in the low-temperature dependencies of $I(T)$. Note that the chemical compositions, T_g, viscosities, and growth rates of the new

and old glasses are close, which is also observed by the coincidence of the nucleation rates at high temperatures, which then justifies data comparison.

Note that well-defined linear parts can be observed at the $N(t)$ dependencies in Figure 5, which are especially accentuated at $T = 719$K and 748 K. It is clear that these linear parts cannot be well described by a smooth function, Eq. (21), for the evolution of the structural parameter. A similar behavior of the N vs t curve for lithium disilicate glass below the glass-transition temperature was shown in Ref. 11 and interpreted as a stepwise relaxation. The possibility of the existence of such long, linear sections on the dependence $N(t)$ until the ultimate steady-state nucleation rate is reached is most probably the reason for the premature termination of the common nucleation experiments, which lead to underestimating the steady-state nucleation rate.

A rather interesting feature of nucleation dynamics revealed in this study, shown by Figure 8, which was not emphasized previously, is that the *actual* temperature of maximum nucleation rate, T_{tmax}, is well *below* the often-reported experimental value. For the current glass, the actual value is ~30 to 60 K below the reported experimental values.

6 | CONCLUSIONS

In this article, we extended the previous analysis performed for lithium disilicate[11] by including the effect of relaxation on the diffusivity and tested the proposed model with another glass-forming system. Our analysis of new and old experimental data sets for a $2Na_2O{\cdot}CaO{\cdot}3SiO_2$ glass at sufficiently low temperatures shows that structural relaxation significantly affects the nucleation dynamics. The effect is particularly notable at temperatures close and below T_g, and results in a continuous increase in the nucleation rate over time. Eventually, the ultimate steady-state value is reached, which corresponds to the time required by the SCL to be fully relaxed at any given temperature. This time is two to three orders of magnitude *longer* than the average relaxation time estimated by the Maxwell relation using viscosity, and experimentally evaluated by refractive index measurements.

The proposed mechanism and model also explain the alleged breakdown of CNT at low temperatures. It is merely because most researchers did not prolong nucleation treatments enough to complete the glass relaxation process and reach the steady-state regime. Another remarkable result is that the actual maximum nucleation temperature, T_{tmax}, is significantly *lower* than the previously reported experimental values. Finally, we present a pertinent comparative analysis of the kinetic coefficient using viscosity versus growth velocity, which favors the last.

These soda-lime-silica glass results extend, validate, and generalize recent findings for lithium disilicate on the significant—but often neglected—effect of relaxation on crystal nucleation. They clearly show that relaxation must be taken into account for a proper analysis of crystal nucleation, mostly below the glass-transition interval.

ACKNOWLEDGMENTS

We are thankful to Coordenação de Aperfeiçoamento de Pessoal de Nível Superior - (CAPES), grant number 88887.468838/2019-00, National Council for Scientific and Technological Development (CNPq), grant number 141816/2018-0 (LRR), and São Paulo Research Foundation (FAPESP), Cepid Project # 2013/007793-6, for the financial support received. This study was financed in part by the Coordenação de Aperfeiçoamento de Pessoal de Nível Superior - Brasil (CAPES) - Finance Code 001.

ORCID

Lorena R. Rodrigues https://orcid.org/0000-0002-7270-6040
Alexander S. Abyzov https://orcid.org/0000-0002-1975-7586
Vladimir M. Fokin https://orcid.org/0000-0001-5966-693X
Edgar Dutra Zanotto https://orcid.org/0000-0003-4931-4505

REFERENCES

1. Holand W, Beall G. Glass-Ceramic Technology. 3rd ed. Wiley; 2019:1–448. https://www.wiley.com/en-us/Glass+Ceramic+Technology%2C+3rd+Edition-p-9781119423706.
2. Deubener J, Allix M, Davis MJ, Duran A, Höche T, Honma T, et al. Updated definition of glass-ceramics. J Non-Cryst Solids. 2018;501:3–10.
3. Kelton KF, Greer AL. Nucleation in Condensed Matter. Applications in Materials and Biology. Pergamon Materials Series. Vol. 15. 1st ed. Elsevier; 2010:1–756.
4. Abyzov AS, Fokin VM, Zanotto ED. Predicting homogeneous nucleation rates in silicate glass-formers. J Non-Cryst Solids. 2018;500:231–4.
5. Abyzov AS, Fokin VM, Yuritsyn NS, Rodrigues AM, Schmelzer JWP. The effect of heterogeneous structure of glass-forming liquids on crystal nucleation. J Non-Cryst Solids. 2017;462:32–40.
6. Fokin VM, Abyzov AS, Zanotto ED, Cassar DR, Rodrigues AM, Schmelzer JWP. Crystal nucleation in glass-forming liquids: variation of the size of the "structural units" with temperature. J Non-Cryst Solids. 2016;447:35–44.
7. Gupta PK, Cassar DR, Zanotto ED. Role of dynamic heterogeneities in crystal nucleation kinetics in an oxide supercooled liquid. J Chem Phys. 2016;145(21):1–211920.
8. Cassar DR, Serra AH, Peitl O, Zanotto ED. Critical assessment of the alleged failure of the Classical Nucleation Theory at low temperatures. J Non-Cryst Solids. 2020;547:120297.
9. Xia X, van Hoesen DC, McKenzie ME, Youngman RE, Kelton KF. The low-temperature nucleation rate anomaly in silicate glasses is an artifact. arXiv. 2005;04845.
10. Acosta HR, Rodrigues LR, Cassar DR, Montazerian M, Peitl O, Zanotto ED. New evidence against the alleged failure of the classical nucleation theory at low temperatures. J Am Ceram Soc. 2021;submitted.
11. Fokin VM, Abyzov AS, Yuritsyn NS, Schmelzer JWP, Zanotto ED. Effect of structural relaxation on crystal nucleation in glasses. Acta Mater. 2021;203:116472.

12. Schmelzer JWP, Tropin TV, Fokin VM, Abyzov AS, Zanotto ED. Effects of glass transition and structural relaxation on crystal nucleation: theoretical description and model analysis. Entropy. 2020;22:1098.
13. Fokin VM, Zanotto ED, Yuritsyn NS, Schmelzer JWP. Homogeneous crystal nucleation in silicate glasses: a 40 years perspective. J Non Cryst Solids. 2006;352:2681–714.
14. DeHoff RT. Quantitative Microscopy. McGraw-Hill Book Company; 1968.
15. Gutzow IS, Schmelzer JWP. The Vitreous State: Thermodynamics, Structure, Rheology, and Crystallization, First edition, Springer, Berlin, 1995; Second enlarged edition, Springer, Heidelberg, 2013.
16. Abyzov AS, Schmelzer JWP, Fokin VM, Zanotto ED. Crystallization of supercooled liquids: self-consistency correction of the steady-state nucleation rate. Entropy. 2020;22(5):1–28.
17. Uhlmann DR. Crystal growth in glass-forming systems: a ten-year perspective. In: Simmons JH, Uhlmann DR, Beall GH editors. Advances in Ceramics, V. 4. Nucleation and crystallization in glasses. Columbus, OH: American Ceramic Soc Inc, 1982; p. 80-124.
18. Abyzov AS, Fokin VM, Rodrigues AM, Zanotto ED, Schmelzer JWP. Effect of elastic stress on the thermodynamic barrier for crystal nucleation. J Non-Cryst Solids. 2017;432:325–33.
19. Fokin VM, Abyzov AS, Zanotto ED, Cassar DR, Rodrigues AM, Schmelzer JWP Crystal nucleation in glass-forming liquids: effect of the size of the "structural units". J Non-Cryst Solids. 2016;447:35–44.
20. Kalinina AM, Filipovich VN, Fokin VM. Stationary and non-stationary crystal nucleation rate in a glass of $2N_2O{\cdot}CaO{\cdot}3SiO_2$ stoichiometric composition. J Non-Cryst Solids. 1980;38–39:723–28. https://doi.org/10.1016/0022-3093(80)90522-0. Fokin VM. Ph.D. dissertation, Silicate Chemistry Institute. Leningrad, 1980 (in Russian);
21. Schmelzer JWP, Abyzov AS, Fokin VM, Schick C, Zanotto ED. Crystallization in glass-forming liquids: Effects of decoupling of diffusion and viscosity on crystal growth. J Non-Cryst Solids. 2015;429:45–53.
22. Nascimento MLF, Zanotto ED. Does viscosity describe the kinetic barrier for crystal growth from the liquidus to the glass transition? J Chem Phys. 2010;133:174701.
23. Lancelotti RF, Cassar DR, Nalin M, Peitl O, Zanotto ED. Is the structural relaxation of glasses controlled by equilibrium shear viscosity? J Am Ceram Soc. 2020; https://doi.org/10.1111/jace.17622.
24. Kashchiev D. Solution of the non-steady state problem in nucleation kinetics. Surf Sci. 1969;14:209–20.
25. Fokin VM, Schmelzer JWP, Nascimento MLF, Zanotto ED. Diffusion coefficients for crystal nucleation and growth in deeply undercooled glass-forming liquids. J Chem Phys. 2007;126:234507.

How to cite this article: Rodrigues LR, Abyzov AS, Fokin VM, Zanotto ED. Effect of structural relaxation on crystal nucleation in a soda-lime-silica glass. *J Am Ceram Soc*. 2021;104:3212–3223. https://doi.org/10.1111/jace.17765

APPENDIX

Comparative analyses of nucleation kinetics using viscosity and growth velocity

Researchers often analyze crystal nucleation kinetics assuming that the diffusion coefficient D_η calculated from the shear viscosity, η, describes the transport process controlling nucleation. In fact, at first glance, a visual analysis of Figure A1 shows that the temperature dependence of the nucleation rate is better described using D_η than the D_U of crystal growth velocity, U (which was employed in the present paper). The data points of Figure A1 show the nucleation rates corresponding to the final parts of the experimental N vs t curves. The blue and magenta solid lines were numerically simulated based on the *cluster dynamics model* with D_U and D_η, respectively.

The proximity of the experimental blue rhombuses to the magenta curve could be interpreted as the achievement of a steady-state nucleation rate and, hence, that viscosity describes the nucleation rates. However, this conclusion would be *incorrect* as we will show below. One should recall that the first step

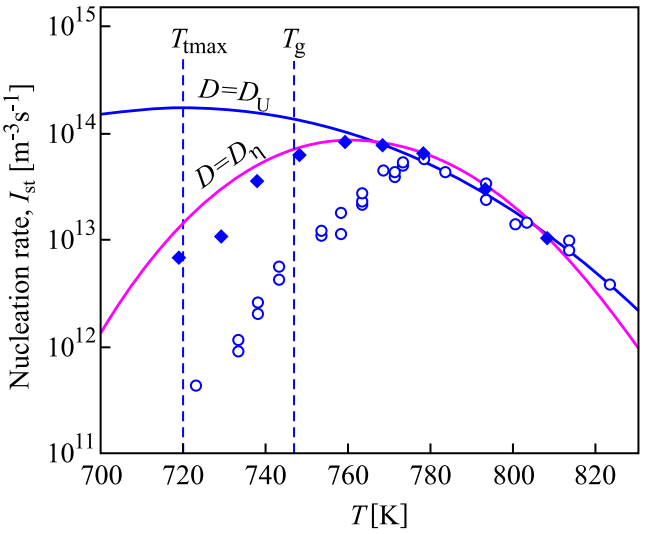

FIGURE A1 Theoretical and experimental nucleation curves. The blue and magenta curves were simulated using $D_U$and D_η, respectively. Rhombuses and circles denote experimental new (prolonged times) and old literature data, respectively. T_{tmax}refers to curve simulated, using D_U [Color figure can be viewed at wileyonlinelibrary.com]

TABLE A1 D and σ estimated as fit parameters given the best description of the final parts of the experimental dependences $N(t)$ in the framework of Cluster Dynamics Model and nucleation rates $I = dN/dt$ corresponding to these parts.

T [K]	I [mm^{-3}s^{-1}]	σ [J/m^2]	D [m^2/s]
719	6749	0.0781	$5.30 \cdot 10^{-24}$
729	10779	0.0795	$1.58 \cdot 10^{-23}$
738	35263	0.0796	$6.97 \cdot 10^{-23}$
748	63295	0.0803	$3.10 \cdot 10^{-22}$
759	83359	0.0807	$8.32 \cdot 10^{-22}$
768	76734	0.0811	$1.57 \cdot 10^{-21}$
778	64239	0.0827	$1.17 \cdot 10^{-20}$
793	29235	0.0843	$6.46 \cdot 10^{-20}$
808	10206	0.0859	$3.57 \cdot 10^{-19}$

towards the analysis of nucleation kinetics is the construction and proper description of the $N(t)$ dependence. The experimental dependence $N(t)$ for $T = 719$K is shown in Figure A2 together with the $N(t)$ calculated using D_η and D_U. It is clear that the experimental data *cannot* be described by CNT without taking into account the glass relaxation process, that is, with $\zeta = 1$.

However, taking relaxation, ζ(t), into account allows us to describe the experimental data with D_U (see solid blue line in Figure A2), as in the present work (Figure 5A), whereas using D_η does not allows us to describe the experimental $N(t)$ curve. One of the attempts is shown in Figure A2 with a dash-dotted line.

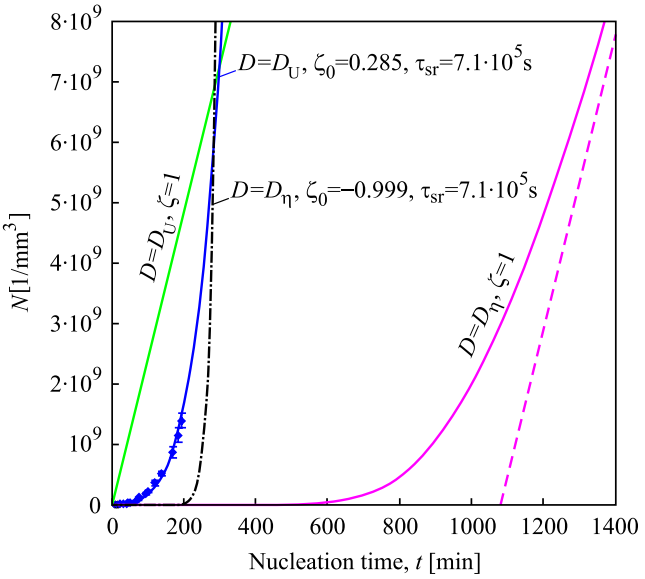

FIGURE A2 Number of crystals per unit volume vs. nucleation time at $T = 719$K. The blue points represent experimental data, whereas the magenta and green lines were simulated using D_η and D_U, respectively, without taking into account the glass relaxation process ($\zeta = 1$). The blue solid line ($D = D_U$) and the black dot-dashed line ($D = D_\eta$) show the simulations taking into account the relaxation process, ζ (t), with D_U and D_η respectively. The fitting parameters are denoted close to the respective lines. The dashed magenta line shows the asymptote, the ultimate steady-state, to the continuous magenta line [Color figure can be viewed at wileyonlinelibrary.com]